



Research Article

Ginseng-derived type I rhamnogalacturonan polysaccharide binds to galectin-8 and antagonizes its function

Yi Zheng^a, Yunlong Si^a, Xuejiao Xu^a, Hongming Gu^a, Zhen He^a, Zihan Zhao^a, Zhangkai Feng^a, Jiyong Su^a, Kevin H. Mayo^b, Yifa Zhou^{a,*}, Guihua Tai^{a,*}

^a Engineering Research Center of Glycoconjugates Ministry of Education, Jilin Provincial Key Laboratory of Chemistry and Biology of Changbai Mountain Natural Drugs, School of Life Sciences, Northeast Normal University, Changchun, China

^b Department of Biochemistry, Molecular Biology and Biophysics, University of Minnesota, Minneapolis, MN, USA



ARTICLE INFO

Keywords:

Pectin
Rhamnogalacturonan I
Galectin-8
Galactan
Interaction

ABSTRACT

Background: *Panax ginseng* Meyer polysaccharides exhibit various biological functions, like antagonizing galectin-3-mediated cell adhesion and migration. Galectin-8 (Gal-8), with its linker-joined N- and C-terminal carbohydrate recognition domains (CRDs), is also crucial to these biological processes, and thus plays a role in various pathological disorders. Yet the effect of ginseng-derived polysaccharides in modulating Gal-8 function has remained unclear.

Methods: *P. ginseng*-derived pectin was chromatographically isolated and enzymatically digested to obtain a series of polysaccharides. Biolayer Interferometry (BLI) quantified their binding affinity to Gal-8, and their inhibitory effects on Gal-8 was assessed by hemagglutination, cell migration and T-cell apoptosis.

Results: Our ginseng-derived pectin polysaccharides consist mostly of rhamnogalacturonan-I (RG-I) and homogalacturonan (HG). BLI shows that Gal-8 binding rests primarily in RG-I and its β -1,4-galactan side chains, with sub-micromolar K_D values. Both N- and C-terminal Gal-8 CRDs bind RG-I, with binding correlated with Gal-8 mediated function.

Conclusion: *P. ginseng* RG-I pectin β -1,4-galactan side chains are crucial to binding Gal-8 and antagonizing its function. This study enhances our understanding of galectin-sugar interactions, information that may be used in the development of pharmaceutical agents targeting Gal-8.

1. Introduction

Polysaccharides are the most abundant, bioactive components in *P. ginseng*, exhibiting e.g. immune-modulation, as well as anti-tumor, anti-adhesive, anti-oxidant and hypoglycemic activities [1–5]. Water-extracted polysaccharides from *P. ginseng* root mainly contain starch-like glucans and pectin [6,7]. Ginseng pectin is composed primarily of galacturonic acid (GalA), rhamnose (Rha), galactose (Gal), arabinose (Ara), and small amounts of other sugars like glucose (Glc) and glucuronic acid (GlcA), that form distinct structural domains, among which homogalacturonan (HG) and type I rhamnogalacturonan (RG-I) are the most abundant. HG has a linear backbone comprised of α -1,4-linked-D-galacturonic acid residues that can be decorated with acetyl groups at the O-2/3 or carbomethoxy C-6 positions [6–9]. RG-I has a backbone of repeating disaccharide units of [α -D-GalA-1,

2- α -L-Rha-1,4-] $_n$ with arabinan, galactan, or arabinogalactan sequence substitutions at the Rha C-4 position [6–9]. Although identifying molecular targets of ginseng pectin has been challenging for researchers, the recent discovery that pectins bind galectins has advanced the field [10].

Galectins are a family of β -galactoside-binding lectins that have a conserved carbohydrate recognition domain (CRD). Galectins have 16 members that are involved in various cellular functions, such as cell adhesion, cell signaling, and apoptosis with consequent effects on cancer, inflammation, and immunity [11–13]. Since the discovery that a modified citrus pectin binds galectin-3 (Gal-3), a number of pectic polysaccharides from different plants has been reported to bind Gal-3 and antagonize function [14–22]. Nevertheless, information on binding of other galectins is minimal. In this study, we focus on pectin interaction with galectin-8 (Gal-8).

* Corresponding authors. Engineering Research Center of Glycoconjugates Ministry of Education, Jilin Provincial Key Laboratory of Chemistry and Biology of Changbai Mountain Natural Drugs, School of Life Sciences, Northeast Normal University, Changchun 130024, China.

E-mail addresses: zhouyf383@nenu.edu.cn (Y. Zhou), taigh477@nenu.edu.cn (G. Tai).

<https://doi.org/10.1016/j.jgr.2023.11.007>

Received 29 July 2023; Received in revised form 27 November 2023; Accepted 29 November 2023

Available online 6 December 2023

1226-8453/© 2024 The Korean Society of Ginseng. Publishing services by Elsevier B.V. This is an open access article under the CC BY-NC-ND license (<http://creativecommons.org/licenses/by-nc-nd/4.0/>).

Gal-8 is a 34 kDa lectin with two homologous (38 % identity) CRDs joined by a linker peptide (~26 amino acids) [23]. The C-terminal CRD preferentially recognizes blood group antigens and poly-LacNAc glycans, whereas the N-terminal CRD prefers to interact with sialylated and sulfated glycans [24,25]. Like other galectins, Gal-8 is synthesized in the cytoplasm and exocytosed via a non-classical secretory pathway [23]. Extracellular Gal-8 binds to cell surface glycoconjugates and components of the extracellular matrix via its CRDs, thereby promoting its function, e.g. angiogenesis [26], and leukocyte and synovial cell apoptosis [27,28]. There are only a few reports on Gal-8-pectin interactions [29], and one report has even argued against Gal-8 binding to pectin [30].

Targeting galectins has been proposed as the basis for pectin-based biological activities. Our previous study showed that ginseng pectin interacts with Gal-3 to modify the lectin's function [18,20]. In the present study we demonstrated that ginseng pectin binds to Gal-8 and antagonizes its function.

2. Materials and methods

2.1. Materials

Sepharose CL-6B and Sephadex G-25 are from Amersham Pharmacia. Pectinase (*Aspergillus niger* endo-PG) is from Sigma-Aldrich. Water-soluble polysaccharide from *P. ginseng* (WGP) is from Shengshengyugu Co. (Liaoning, China).

2.2. RG-I and HG pectins

Ginseng-derived polysaccharide preparation is outlined in Fig. 1A. Water-soluble ginseng polysaccharide (WGP) extracted from ginseng root was loaded onto a DEAE-Cellulose column (8 × 30 cm) and eluted with distilled water to remove the non-binding material [6]. The bound material (referred to as WGPA) was eluted with 0.5 M NaCl, dialyzed against distilled water and lyophilized [6]. WGPA (15 g) was applied to a DEAE-Cellulose column (8 × 30 cm), eluted stepwise with NaCl at 0, 0.1, 0.2, 0.3 and 0.5 M to obtain five fractions (Fig. S1A): WGPA-N (2.5 g), WGPA-1 (1.25 g), WGPA-2 (5.75 g), WGPA-3 (2.94 g) and WGPA-4 (1.07 g).

For RG-I- and HG-rich pectins, WGPA-2 (4 g) and WGPA-3 (2 g) were separated into fractions 2A (0.81 g), 2B (2.78 g), 3A (0.31 g) and 3B (1.55 g) by gel-permeation chromatography (Sepharose CL-6B column, 2.6 × 100 cm) (Fig. S1B, C).

To enrich RG-I domains, 2A (500 mg), 3A (200 mg), 2B (1 g) and 3B (1 g) were dissolved (10 mg/mL) in sodium acetate buffer and digested with Endo-PG (30 mU/mg) at 50 °C for 2 h. Digests were applied to Sephadex G-25 columns (5 × 30 cm) and eluted (2 mL/min) with distilled water. Void volume eluates yielded fractions 2A-D (324 mg), 3A-D (132 mg), 2B-D (341 mg) and 3B-D (430 mg).

To purify 2A-D, 250 mg was applied to Sepharose CL-6B columns (1.6 × 100 cm) and eluted with 0.15 M NaCl (0.15 mL/min). Recovered polysaccharide peak was dialyzed and lyophilized to yield 223 mg 2A-Dp.

For partial acid hydrolysis, 150 mg (3 parts, 50 mg) 2A-Dp was dissolved (10 mg/mL) in 0.1 M TFA, and hydrolyzed at 80 °C for 1, 4 and 12 h, respectively. pH was adjusted (pH 6.5–7.5) using 10 % ammonium hydroxide, after which hydrolysates were applied to Sephadex G-25 columns (5 × 30 cm) and eluted with distilled water. Void volume eluates yielded 28 mg Core-1, 22 mg Core-2 and 18 mg Core-3. Sugar compositions and weight-averaged molecular weights were determined as described previously [6].

2.3. NMR spectroscopy

Polysaccharides (20 mg) were dissolved in 0.5 mL D₂O (99.8 %) and stirred overnight. Natural abundance ¹³C NMR spectra (15,000 scans),

as well as ¹H-¹³C HMBC and HSQC spectra, were acquired at 25 °C using a 5 mm broadband probe on a Bruker AV600 spectrometer (Karlsruhe, Germany). Data were processed using standard Bruker software.

2.4. Preparation of recombinant Gal-8 and its variants

The Gal-8 gene was synthesized by SynBio Technologies (Jiangsu, China). Full-length Gal-8 (1–317 residues) and its CRDs (N-CRD, 19–152 residues; C-CRD, 187–317 residues) genes were cloned into pET28a-vectors (Novagen). Plasmids were prepared using QuickChange XL site-directed mutagenesis kits (Stratagene).

For protein expression, constructs were transfected into *E. coli* BL21 (DE3) cells and grown in LB medium with kanamycin (100 µg/mL). When the OD₆₀₀ reached 0.6–0.8, IPTG was added to 0.5 mM. Recombinant proteins (His-tagged) were isolated from cell lysates and purified using Ni-NTA agarose beads as described previously [31]. Protein purity was determined by SDS-PAGE (Fig. S2).

2.5. Gal-8-mediated hemagglutination (G8H)

This assay was performed as described previously [32] with some modifications such that each ice-chilled V-plate well contained 25 µL (4 % v/v) chicken erythrocytes and 75 µL Tris-HCl buffer (10 mM, 150 mM NaCl, pH 8.0) with or without Gal-8 and polysaccharide. Cell suspensions were then added, followed by mild shaking. Plates sat 60 min undisturbed on ice. Minimum inhibitory concentration (MIC) was determined by examining diluted polysaccharide samples.

2.6. Biolayer interferometry (BLI)

Affinity for Gal-8 and variants was assessed using ForteBio Octet RED 96 instrument (California, USA) and Ni-NTA biosensors, with proteins and pectins dissolved in TBST (10 mM Tris-HCl, 150 mM NaCl, 0.2 % Tween-20, pH 7.5). Program was: initial baseline 60 s, loading in 5 µg/mL His-tagged Gal-8, variants or TBST (control) 100 s, baseline 60 s, association with pectins 60 s, and dissociation in buffer 60 s. For non-specific binding, samples were examined without polysaccharides in the loading step. For binding kinetics, five concentrations of each sample were tested, with binding parameters analyzed using ForteBio Data Analysis Software 8.0.

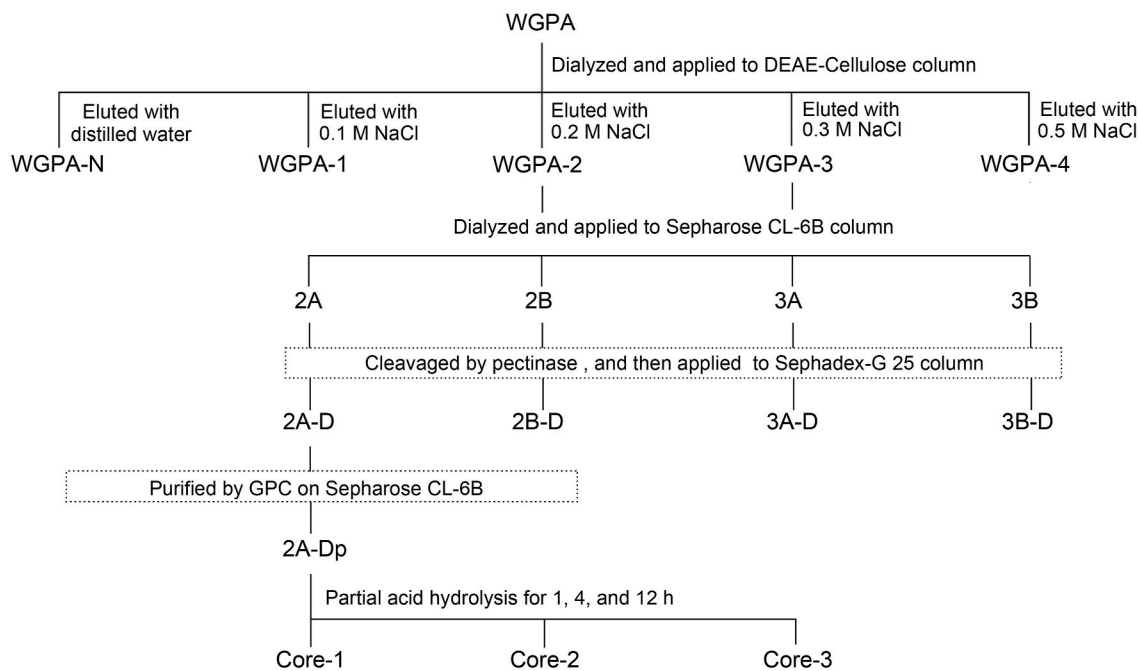
2.7. Gal-8-mediated T cell apoptosis

Jurkat cells (10⁶ cells/well) in serum free medium were seeded in 12-well plates and co-cultured with 0.6 µM Gal-8 for 18 h. For inhibition assessment, Gal-8 was mixed with lactose, sucrose or 2A-Dp (30 min), and mixtures were added to cells. Apoptosis was assessed by western blotting for active form of caspase-3 (cleaved-caspase) and PARP (cleaved-PARP) [33]. Inhibition was quantified using 2 × 10⁶ Jurkats treated with 0.6 µM Gal-8 for 18 h at 37 °C with and without 0.5 mg/mL lactose, sucrose, 2A-Dp, Core-1 or Core-2. Following treatment, cells were re-suspended in 100 µL binding buffer, and Annexin V-FITC (5 µL) and PI (5 µL) were added and incubated for 15 min in the dark. Number of apoptotic cells was assessed using BD Accuri™ C6 flow cytometer.

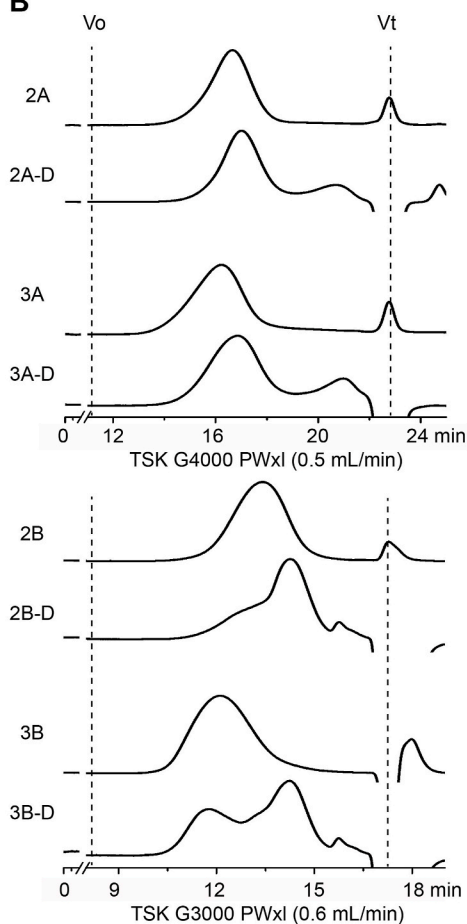
2.8. Cell migration

Real-time measurements were performed using xCELLigence RTCA DP instrument (Roche Diagnostics, Mannheim, Germany). HMEC-1 cells were trypsin digested and re-suspended in MCDB131 serum-free medium. 10⁶ HMEC-1 cells were seeded/well in CIM-plate upper chambers (Roche Diagnostics) that were then placed onto lower parts of the CIM-device. In lower chambers, serum-free MCDB131 or 0.3 µM Gal-8 was used with or without sugars. Migration was followed for 13 h by monitoring changes in impedance signals on CIM-plates as described for xCELLigence SP systems. Data acquisition/analysis were performed

A



B



C

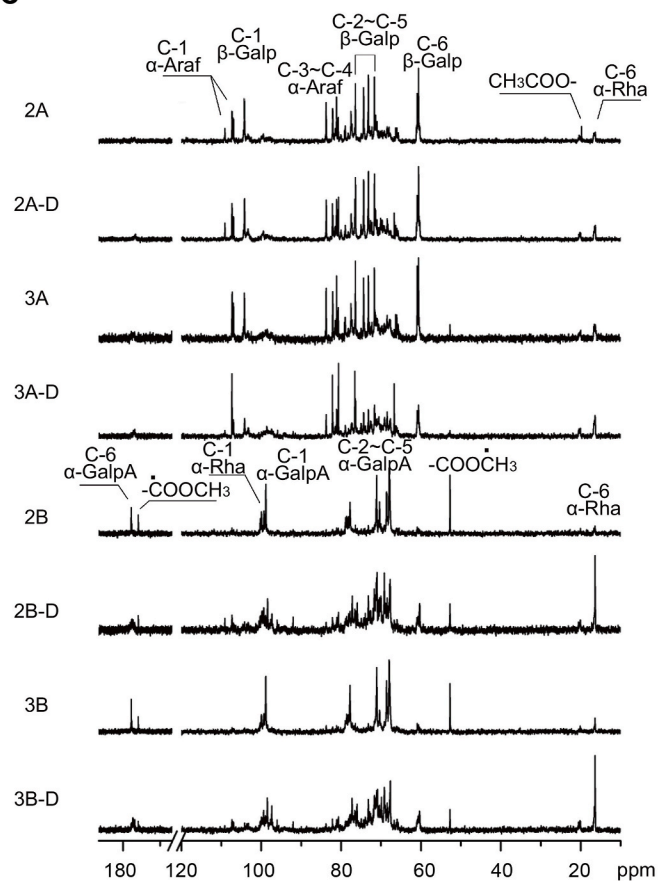


Fig. 1. Ginseng pectin fractions. **A.** Preparation scheme. **B–C.** HPGPC chromatograms (**B**) and ¹³C NMR spectra (**C**) of pectin fractions.

using RTCA software (v1.2, Roche Diagnostics).

2.9. Statistical analysis

Results are expressed as the mean \pm standard deviation of at least three independent experiments. Statistical significance was assessed by the Student's *t*-test between two groups in SPSS 23.0 (IBM, Armonk, USA). **p* < 0.05, ***p* < 0.01, ****p* < 0.001.

3. Results

3.1. Polysaccharide structural features

Fig. 1 shows the polysaccharide separation scheme (Fig. 1A), as well as the assessment of their molecular weight (Fig. 1B) and chemical structure (Fig. 1C).

3.2. Fractions 2A, 2B, 3A, 3B

Fractions 2A, 2B, 3A and 3B are homogenous with single peaks at 98, 10, 137 and 39 kDa, respectively (Fig. 1B). 2A and 3A have relatively high Rha/GalA ratios (0.75 and 0.52, respectively) and high contents of Gal and Ara (Table S1), suggesting that these fractions contain RG-I [34]. In contrast, 2B and 3B show low Rha/GalA ratios (0.07 and 0.08, respectively), yet high contents of GalA (73.4 % and 74.7 %, respectively), indicating that these primarily contain HG.

2A and 3A display similar ^{13}C NMR spectra (Fig. 1C), with anomeric carbon-signals for 1,5-/1,3,5-linked α -Araf (~107 ppm) and β (1 \rightarrow 4)-linked Galp (~104 ppm), i.e. common structural components of RG-I side chains. Methyl signals of α -1,2- and α -1,2,4-Rha (16–17 ppm) are also typical of RG-I backbone [35,36]. HG-rich pectins 2B, 3B display similar NMR spectra, with resonances corresponding to carbonyl carbons of un-esterified (~175 ppm) and esterified (~171 ppm) GalA, as well as methoxycarbonyl-carbons (52.7 ppm) and anomeric-carbons (97–99 ppm) of GalA being dominant [7].

3.3. Fractions 2A-D, 2B-D, 3A-D, 3B-D

2A-D, 2B-D, 3A-D, 3B-D were derived from 2A, 2B, 3A and 3B, respectively, by disrupting HG domains. Rha/GalA ratios (Table S1) in 2A-D (0.81) and 3A-D (0.73) are greater than in 2A (0.75) and 3A (0.52), confirming enhanced RG-I content. 2B-D and 3B-D display two major peaks on HPGPC (Fig. 1C), suggesting two populations in parental material 2B and 3B, with one population being mostly insensitive to pectinase. Nevertheless, RG-I content is enriched in 2B-D and 3B-D, as indicated by increased Rha/GalA ratios (0.5 for 2B-D vs 0.07 for 2B; 0.36 for 3B-D vs 0.08 for 3B) (Table S1).

^{13}C NMR spectra of 2A-D (Fig. 1C) are similar to that of 2A, and 3A-D signals are also observed in 3A, although relative intensities of some signals in 3A-D differ. Increased Rha (16–17 ppm) and decreased GalA (~175, ~171, 52.7 and 97–99 ppm) ^{13}C NMR signal intensities are consistent with enhanced RG-I content in 2B-D and 3B-D (Fig. 1C).

3.4. Fragments 2A-Dp, Core-1, Core-2 and Core-3

Purified 2A-D fragment 2A-Dp was partially hydrolyzed giving fragments Core-1, Core-2 and Core-3 (Fig. 1A), with sizes decreasing from 2A-Dp (75 kDa) to Core-1 (58 kDa), Core-2 (37 kDa) and Core-3 (22 kDa), but as single peaks up to Core-2 (Fig. 2A). This suggests that terminal residues are gradually hydrolyzed from 2A-Dp to Core-2. Conversely, Core-3 shows a dispersed peak, suggesting that its backbone is also altered. Acid-sensitive Ara content rapidly decreased from 29.4 % (2A-Dp) to 10.8 % (Core-1), 3.0 % (Core-2), and 0.9 % (Core-3) (Table S1), whereas Gal content was 39.9 % (2A-Dp), 48.1 % (Core-1), 44.1 % (Core-2) and 38.1 % (Core-3). The increase in Core-1 Gal content after 1 h vis-à-vis untreated 2A-Dp results from the decrease in Ara

content.

Structure of 2A-Dp and fragments was investigated by 1D NMR (Fig. 2B) and 2D NMR (Fig. 2C for partial and Fig. S3 for full spectra), with chemical shifts listed in Table S2. In 1D ^{13}C NMR spectra, Ara resonances (C1 109.1 ppm, 107.4 ppm, 107.0 ppm) are the primary signals in 2A-Dp, with intensities markedly decreasing in Core-1 and not observed in Core-2 or Core-3. β -1,4-galactan side chain signals (C1 of β -1, 4-Gal at 104.2 ppm and C1 of β -T-Gal at 103.3 ppm) are the major peaks in all spectra. Signals corresponding to RG-I backbones (i.e. α -1,2-Rha, α -1,2,4-Rha and α -1,4-GalA) are present in all spectra with intensities increasing from 2A-Dp to Core-3. With sugar composition, NMR data indicate that 2A-Dp and fragments all contain RG-I backbones, with branching degrees 42 % 2A-Dp, 46 % Core-2 and 39 % Core-3, estimated from ratios of HC6 signals from α -1,2,4-Rha and α -1,2-Rha (Fig. S3 inserts). Whereas 2A-Dp and Core-1 contain β -1,4-galactan and arabinan (or arabinogalactan) side chains, Core-2 and Core-3 primarily contain β -1,4-galactan side chains. Of note, Core-2 has the smallest core structure with intact RG-I backbone and resonances (Fig. 2C) mostly accounted for by β -1,4-galactan side chains and RG-I backbone. Structure diagrams are shown in Fig. 2D.

3.5. RG-I-rich pectin binds Gal-8 more strongly than HG-rich pectin

Effects of polysaccharides on Gal-8-mediated hemagglutination (G8H) was examined using different concentrations of Gal-8. Because ≥ 1.0 $\mu\text{g}/\text{mL}$ Gal-8 promoted agglutination (Fig. 3A), we used 1.25 $\mu\text{g}/\text{mL}$ Gal-8 in subsequent studies. MIC with lactose was 8 $\mu\text{g}/\text{mL}$, whereas sucrose had no inhibitory effect to 500 $\mu\text{g}/\text{mL}$ (Fig. 3B). MICs with RG-I-rich 2A (42 $\mu\text{g}/\text{mL}$) and 3A (250 $\mu\text{g}/\text{mL}$) were much lower than with HG-rich 2B (466 $\mu\text{g}/\text{mL}$) and 3B (533 $\mu\text{g}/\text{mL}$) (Table 1 and Fig. 3C,D).

Direct binding to Gal-8 was analyzed by Biolayer Interferometry (BLI) where the biosensor was loaded with equal amounts of Gal-8 (5 $\mu\text{g}/\text{mL}$) and dipped into the polysaccharide solution (association) prior to transfer to TBST solution (dissociation). Analysis (Table 1 and Fig. 3E) yielded K_{D} s of 15.4 and 12.5 nM for 2A and 3A, respectively, much lower than for 2B (1,355 nM) and 3B (357 nM). Thus, both G8H and BLI indicate that RG-I-rich polysaccharides interact more strongly with Gal-8.

3.6. Enrichment of RG-I content increases binding

Because RG-I-rich 2A and 3A contain some HG, whereas HG-rich 2B and 3B contain small amounts of RG-I, we wondered whether enrichment of RG portions increases Gal-8 binding. Therefore, we treated fractions with pectinase to degrade HG and observed that digests 2A-D, 3A-D, 2B-D and 3B-D all had higher RG-I content and exhibited greater inhibition than parental fractions in G8H (Fig. 3C,D and Table 1). Also, Gal-8 binding increased (Table 1 and Fig. 3E), indicating that RG-I portions in each polysaccharide bind Gal-8.

3.7. β -1,4-galactan side chains mediate Gal-8 binding

To further investigate Gal-8 and RG-I binding, we used purified RG-I fragment 2A-Dp isolated from the most active 2A-D. Partial acid hydrolysis of 2A-Dp yielded Core-1, Core-2, and Core-3 that gave K_{D} s for Gal-8 (Table 1 and Fig. 3E) of 6.8, 7.5 and 12.8 nM, respectively, similar to parent 2A-Dp (11.3 nM). Because Core-2 and Core-3 primarily contain β -1,4-galactan side chains and few Ara residues unlike 2A-Dp, and Gal-8 affinities remained high, we proposed that 1) Ara residues contribute little to Gal-8 binding, and 2) β -1,4-galactan side chains are functionally important. In support of this, we found that the Gal-8 K_{D} is increased (indicating weaker binding) to $> 17,000$ nM (Table 1) when the side chains are removed and only the RG-I backbone (i.e. RG-I-RG) is present (Fig. S4).

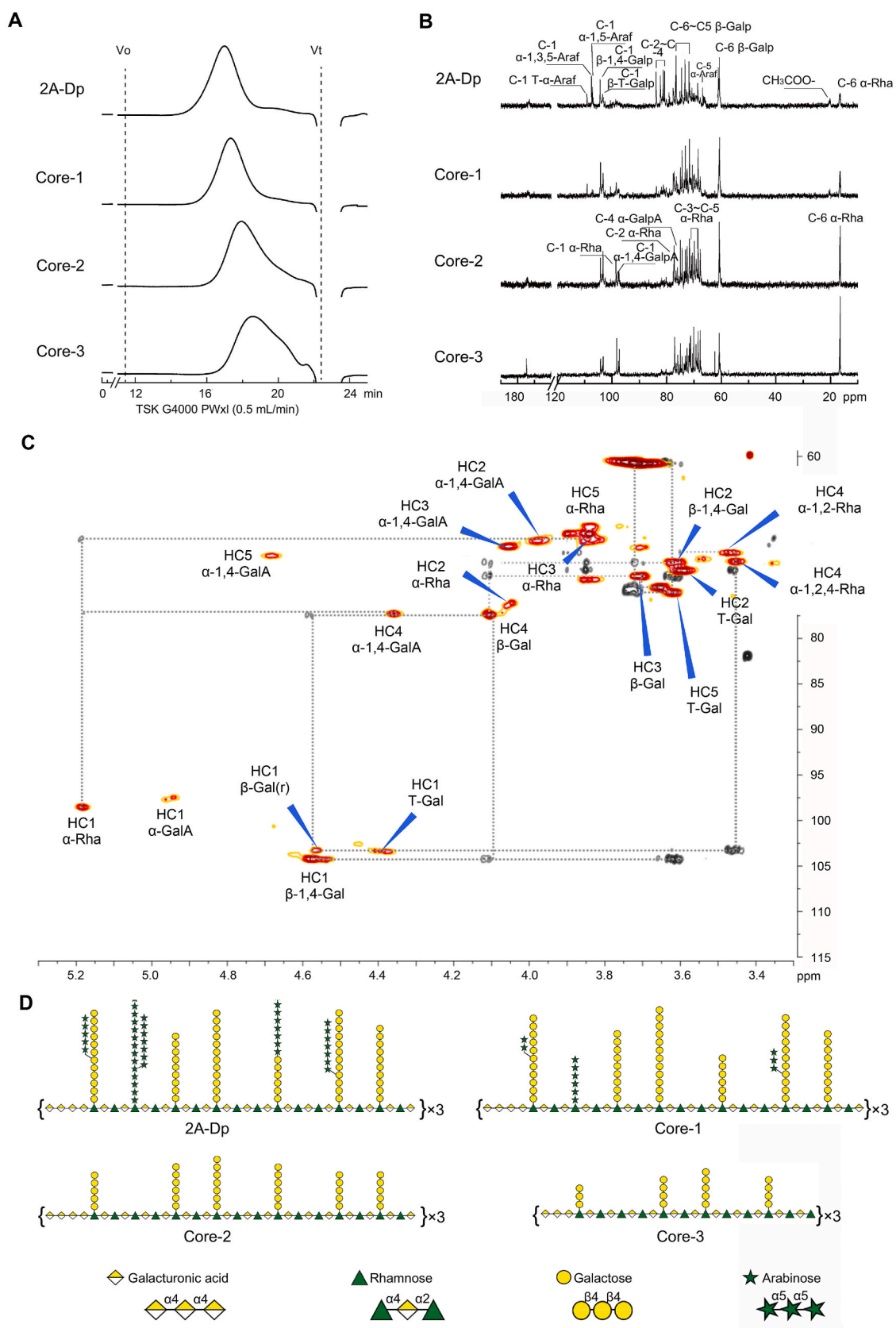


Fig. 2. 2A-Dp and core fragments. **A.** HPGPC chromatograms. **B.** ^{13}C NMR spectra. **C.** Expansions of ^{13}C H- ^{13}C HSQC (red) and HMBC (black) of Core-2. **D.** Structure diagrams.

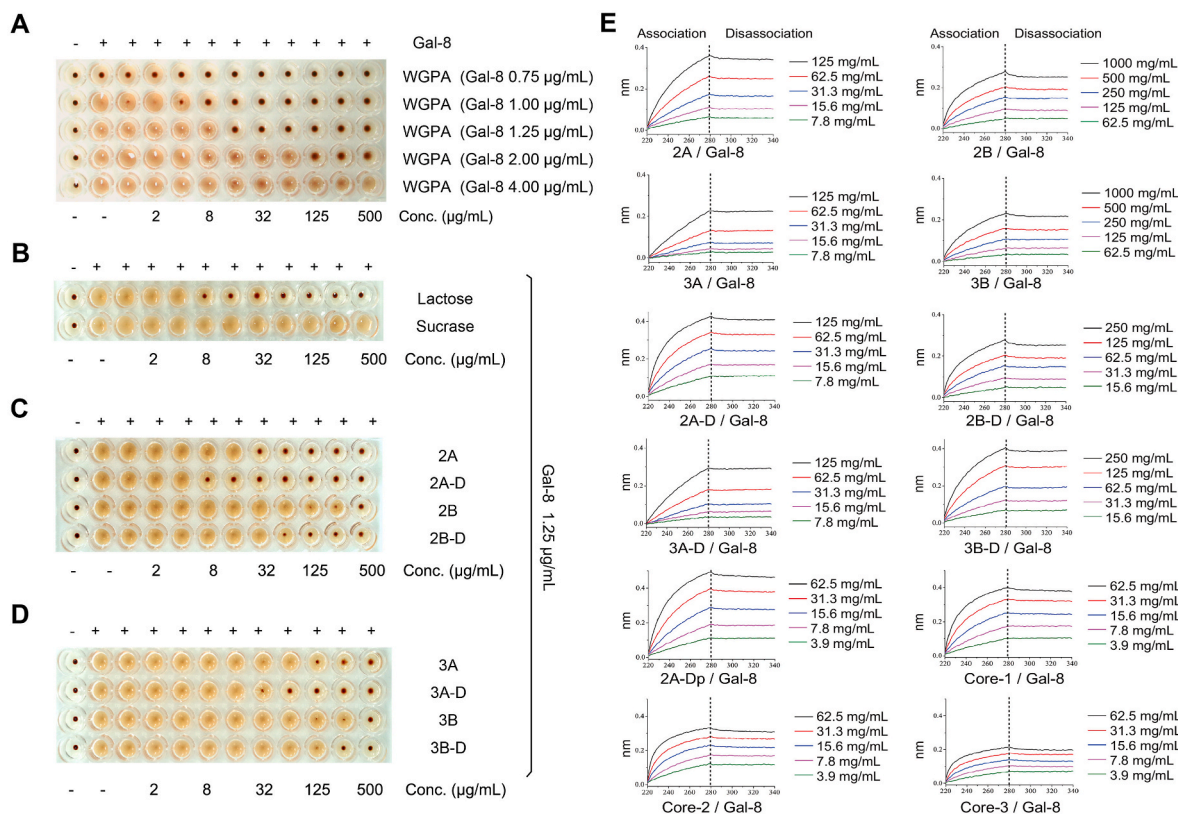


Fig. 3. Interactions between Gal-8 and saccharides. **A-D.** Gal-8-mediated hemagglutination (G8H). **A.** Optimization of conditions with WGPA and Gal-8 concentrations. **B-D.** Inhibition of 1.25 µg/mL Gal-8-mediated hemagglutination by lactose (positive control), sucrose (negative control) and polysaccharides. **E.** BLI assay. Increasing concentrations of pectin-derived fractions were examined using Ni-NTA sensors immobilized Gal-8. Association/dissociation steps are shown.

Table 1
Weight-averaged molecular weights (Mw), MIC and dissociation constants (K_D).

Pectin	Mw (kDa)	MIC		K _D from BLI	
		(nM)	(µg/mL)	(nM)	(µg/mL)
WGPA	na	na	21 ± 9	na	0.61 ± 0.08
2A	98	430 ± 184	42 ± 18	15.4 ± 5.5	1.51 ± 0.31
2A-D	75	120 ± 80	9 ± 6	11.8 ± 3.6	0.89 ± 0.11
2B	10	46600 ± 5700	466 ± 57	1,355 ± 306	13.55 ± 2.12
2B-D	26/4.3	9082 ± 3057 ^a	104 ± 35	131 ± 28 ^a	1.50 ± 0.23
3A	137	1824 ± 365	250 ± 50	12.5 ± 4.5	1.71 ± 0.42
3A-D	83	627 ± 204	52 ± 17	10.8 ± 4.2	0.90 ± 0.13
3B	39	13666 ± 1460	533 ± 57	357 ± 95	13.92 ± 2.20
3B-D	54/4.4	10770 ± 1290 ^a	233 ± 28	98 ± 12 ^a	2.12 ± 0.48
2A-Dp	75	-	-	11.3 ± 3.2	0.85 ± 0.11
Core-1	58	-	-	6.8 ± 1.5	0.39 ± 0.06
Core-2	37	-	-	7.5 ± 0.9	0.28 ± 0.07
Core-3	22	-	-	12.8 ± 2.5	0.28 ± 0.04
P-galactan ^b	na	-	-	na	9.18 ± 2.1
RG-I-RG ^c	2.7	-	-	>17,000	>45.90

^a Values were calculated using the weight average molecular weight of respective fractions.
^b Potato galactan from Megazyme (cat. P-GALPOT).
^c RG-I backbone prepared according to Gao et al. [18]. na, not applicable. -, not tested. Each value represents the mean ± SD of three independent experiments.

3.8. Polysaccharide binding is Gal-8 CRD-dependent

To investigate which Gal-8 CRD (N- or C-terminal) is involved in binding, we prepared separate N- and C-CRDs (Fig. S2). Here, we observed that 2A-Dp (Fig. 4A,B) bound to N-CRD (K_D = 96 nM) somewhat more strongly than to C-CRD (K_D = 218 nM). Nevertheless, full-length Gal-8 bound best (K_D = 11.3 nM), indicating that both CRDs promote maximal binding. Lactose inhibited binding, more so to N-CRD (IC = 1.25 mM, Fig. 4D) than to C-CRD (IC = 5 mM, Fig. 4E) or to full length Gal-8 (IC = 10 mM, Fig. 4C). Thus, the canonical β-galactoside

binding S-face of both N- and C-CRDs are involved in binding.

3.9. 2A-Dp and core fragments inhibit Gal-8 function

To assess whether Gal-8 binding to these polysaccharides is biologically relevant, we investigated the effect of 2A-Dp on Gal-8-mediated T cell apoptosis, a process implicated in tumor immune escape [37]. Western blotting was used to show cleavage of caspase-3 and PARP (downstream caspase-3 effector). Gal-8-mediated apoptosis was inhibited by lactose (positive control) and 2A-Dp, but not by sucrose (negative

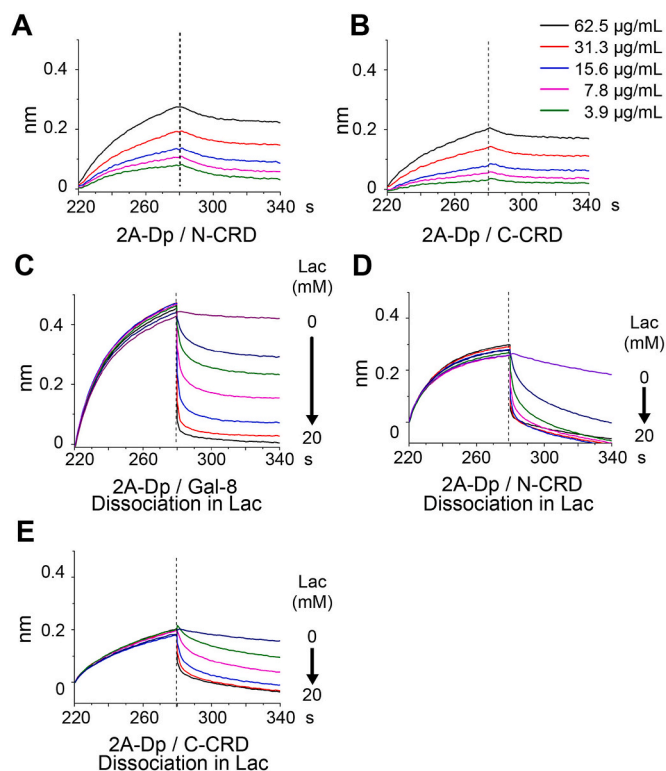


Fig. 4. Polysaccharide-Gal-8/mutant binding by BLI. **A,B.** 2A-Dp binding to N-CRD (**A**), C-CRD (**B**). **C-E.** Lactose inhibits binding of 2A-Dp to full length Gal-8 (**C**), N-CRD (**D**) and C-CRD (**E**). Association step (62.5 $\mu\text{g/mL}$ 2A-Dp) was performed without lactose, and the dissociation step was performed with lactose: 0, 0.63, 1.25, 2.5, 5.0, 10, or 20 mM.

control) (Fig. 5A–D). Inhibition of 2A-Dp (0.5 mg/mL, 6.67 μM) was similar to that from 0.5 mg/mL (1.46 mM) lactose. Flow cytometry with FITC-Annexin V/PI double staining quantified this (Fig. 5E,F). Treatment of Jurkats with 0.6 μM Gal-8 gave ~60 % apoptosis compared to 7 % for untreated cells. Furthermore, 0.5 mg/mL lactose (1.46 mM), but not sucrose, completely inhibited Gal-8-induced apoptosis. 0.5 mg/mL

2A-Dp (6.67 μM) and its core fragments Core-1 (8.62 μM) and Core-2 (13.6 μM) also significantly inhibited apoptosis by ~50 %.

2A-Dp and its core fragments also had an effect on Gal-8-mediated vascular endothelial cell migration (HMEC-1, Fig. 5G,H), a process involved in tumor angiogenesis [26]. The Cell Index (representing cell migration) for Gal-8 increased rapidly to its maximal level in ~6 h, and then slowly decreased up to 13 h. Gal-8 trace was much higher than that of control (no Gal-8), indicating that the presence of Gal-8 promoted migration. Various sugars affected Gal-8-induced cell migration. Whereas lactose inhibited cell migration, sucrose did not. 2A-Dp, Core-1 and Core-2 all showed significant inhibition, albeit not as potently as lactose. At both 0.1 and 0.5 mg/mL, inhibitory effects are Core-2 > Core-1 > 2A-Dp. Notably, comparative inhibition was relative, because the assays were performed at the same mass concentration. At 0.1 mg/mL, corresponding molarities are 290 μM (lactose), 1.33 μM (2A-Dp), 1.72 μM (Core-1) and 2.70 μM (Core-2). At 0.5 mg/mL, the molarities are 1460 μM (lactose), 6.67 μM (2A-Dp), 8.62 μM (Core-1) and 13.5 μM (Core-2). When the assays were performed at the same molar concentrations, e.g. 6.67 μM of lactose (i.e. 2.3 $\mu\text{g/mL}$) or 2A-Dp (i.e. 0.5 mg/mL), lactose was not inhibitory, indicating that the inhibitory activity of 2A-Dp is higher than that of lactose.

4. Discussion

Targeting galectins has been proposed as the basis for pectin-based biological activities, and even though pectin can bind to Gal-3 [14–22], little had been known about pectin binding to Gal-8. One report has even argued against Gal-8 binding to pectin [30]. Here, we used multiple approaches to demonstrate that *P. ginseng* pectins can indeed bind Gal-8 with affinities (or avidities) in sub-micromolar range.

On the structural level, we demonstrated that RG-I pectin binds Gal-8, with the pectin side chain β -1,4-galactans being crucial to that interaction. This conclusion is supported by the following evidence: 1) RG-I-rich pectin binds Gal-8 more strongly than does HG-rich pectin, 2) enhancement of the RG-1 content increases binding, 3) RG-I fragments (Core-2 and Core-3) with only galactan side chains bind strongly, whereas the naked RG-I backbone (i.e. absence of side chains) displays considerably weaker binding (Table 1 and Fig. S4), and 4) commercially available potato galactan (Megazyme, cat. P-GALPOT) also binds Gal-8 ($K_D = 9.18 \mu\text{g/mL}$, Table 1 and Fig. S4). Arabinan side chains in ginseng

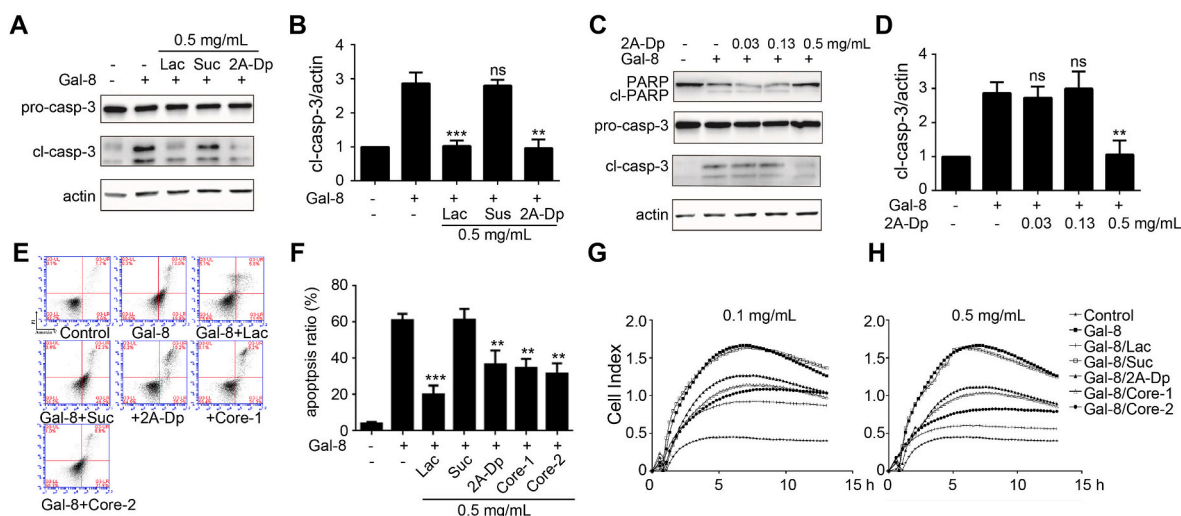


Fig. 5. Inhibition of Gal-8-mediated T cell apoptosis and HMEC-1 migration. **A-D.** Western blotting was performed using an antibody against both intact (pro-casp-3) and cleaved (cl-casp-3) caspase-3, or an antibody against both intact (PARP) and cleaved (cl-PARP) PARP. Actin was the control. **A** and **C.** Representative images. **B** and **D.** Densitometric analysis of ratio of cl-casp-3/actin in **A** and **C**, respectively. Each value represents the mean \pm SD of three independent experiments. Control group was set at 1.0 (i.e. 100 %). **E-F.** Flow cytometry. **E.** Representative images. **F.** Quantification of apoptosis in **E** as mean \pm SD ($n = 3$). **G-H.** Inhibition of Gal-8-mediated HMEC-1 migration with 0.1 mg/mL (**G**) and 0.5 mg/mL (**H**) sugar. ns, not significant. P values were determined using Student's two-tailed *t*-test. ns, not significant. ** $p < 0.01$, *** $p < 0.001$, compared to Gal-8 alone.

RG-I apparently do not contribute to Gal-8 binding, because RG-I fragments with (2A-Dp and Core 1) and without (Core 2 and Core 3) arabinan side chains have similar binding affinities. Furthermore, a commercially available sugar beet arabinan (Megazyme, cat. P-ARAB) barely inhibits G8H (Fig. S5). It is worth noting that the structure of pectin, especially that of RG-I, is quite diverse, and therefore, it is not surprising that pectins from different sources exhibit different Gal-8 binding affinities/avidities. Whereas MCP-3p, a pure HG fraction derived from MCP [38], has no G8H inhibitory effect with Gal-8 up to 2000 µg/mL, PGA from Megazyme (Cat. P-PGACIT) inhibits G8H (MIC = 125 µg/mL) (Fig. S5). Differences between these samples likely relate to differences in their HG content, degree of esterification, and molecular weight, an issue requires further investigation.

Although ginseng polysaccharides are implicated in various pharmaceutical applications, their molecular targets remain unclear. Our previous study showed that ginseng pectin interacts with Gal-3 to modify its function [18,20]. Here, we report that ginseng RG-I pectin binds to Gal-8, thereby inhibiting its function. This finding expands our understanding of how a ginseng-derived polysaccharide operates in situ, therefore, prompting its development as a pharmaceutical agent and dietary supplement.

Several polysaccharide-based inhibitors of Gal-1 and Gal-3 have already been investigated in clinical trials against cancer and fibrotic disease [39,40]. Our present finding extends this list. Moreover, because Gal-8 and Gal-3 exert similar effects on tumor metastasis by promoting endothelial cell migration in angiogenesis and inducing T-cell apoptosis in tumor immunosuppression, ginseng pectins present the prospect of being developed as a more effective inhibitor by blocking both Gal-3 and Gal-8. Our preliminary data show that ginseng pectin also interacts with and inhibits Gal-1, another member of the galectin family that induces T-cell apoptosis. Future investigations will be crucial to unveiling the full potential of ginseng pectins.

In conclusion, we have used multiple approaches here to demonstrate that certain ginseng-derived polysaccharides bind strongly to Gal-8 and inhibit its function. Structure-activity relationships indicate that Gal-8 binds primarily to RG-I, in particular its β-1,4-galactan side chains. Moreover, Gal-8 mutants reveal that both N- and C-terminal CRDs are involved in the binding process.

Declaration of competing interest

The authors declare no conflicts of interest.

Acknowledgements

This work was supported by the National Natural Science Foundation of China (grant numbers 32171276 and 31870796).

Appendix A. Supplementary data

Supplementary data to this article can be found online at <https://doi.org/10.1016/j.jgr.2023.11.007>.

References

- Hu Y, He Y, Niu Z, Shen T, Zhang J, Wang X, Hu W, Cho JY. A review of the immunomodulatory activities of polysaccharides isolated from Panax species. *J Ginseng Res* 2022;46(1):23–32.
- Tao R, Lu K, Zong G, Xia Y, Han H, Zhao Y, Wei Z, Lu Y. Ginseng polysaccharides: potential antitumor agents. *J Ginseng Res* 2023;47(1):9–22.
- Lee JH, Shim JS, Lee JS, Kim MK, Chung MS, Kim KH. Pectin-like acidic polysaccharide from Panax ginseng with selective antiadhesive activity against pathogenic bacteria. *Carbohydr Res* 2006;341(9):1154–63.
- Chen F, Huang G. Antioxidant activity of polysaccharides from different sources of ginseng. *Int J Biol Macromol* 2019;125:906–8.
- Sun C, Chen Y, Li X, Tai G, Fan Y, Zhou Y. Anti-hyperglycemic and anti-oxidative activities of ginseng polysaccharides in STZ-induced diabetic mice. *Food Funct* 2014;5:845–8.
- Zhang X, Yu L, Bi H, Li X, Ni W, Han H, Li N, Wang B, Zhou Y, Tai G. Total fractionation and characterization of the water-soluble polysaccharides isolated from Panax ginseng C. A. Meyer. *Carbohydr Polym* 2009;77(3):544–52.
- Yu L, Zhang X, Li S, Liu X, Sun L, Liu H, Iteku J, Zhou Y, Tai G. Rhamnogalacturonan I domains from ginseng pectin. *Carbohydr Polym* 2010;79(4):811–7.
- Sun L, Ropartz D, Cui L, Shi H, Ralet MC, Zhou Y. Structural characterization of rhamnogalacturonan domains from Panax ginseng C. A. Meyer. *Carbohydr Polym* 2019;203:119–27.
- Wang J, Li S, Fan Y, Chen Y, Liu D, Cheng H, Gao X, Zhou Y. Anti-fatigue activity of the water-soluble polysaccharides isolated from Panax ginseng C. A. Meyer. *J Ethnopharmacol* 2010;130:421–3.
- Glinkov VV, Raz A. Modified citrus pectin anti-metastatic properties: one bullet, multiple targets. *Carbohydr Res* 2009;344(14):1788–91.
- Thijssen VL, Rabinovich GA, Griffioen AW. Vascular galectins: regulators of tumor progression and targets for cancer therapy. *Cytokine Growth Factor Rev* 2013;24(6):547–58.
- Toscano MA, Martinez Allo VC, Cutine AM, Rabinovich GA, Marino KV. Untangling galectin-driven regulatory circuits in autoimmune inflammation. *Trends Mol Med* 2018;24(4):348–63.
- Mendez-Huergo SP, Blidner AG, Rabinovich GA. Galectins: emerging regulatory checkpoints linking tumor immunity and angiogenesis. *Curr Opin Immunol* 2017;45:8–15.
- Inohara H, Raz A. Effects of natural complex carbohydrate (citrus pectin) on murine melanoma cell properties related to galectin-3 functions. *Glycoconjugate J* 1994;11:527–32.
- Nangia-Makker P, Hogan V, Honjo Y, Baccarini S, Tait L, Bresalier R, Raz A. Inhibition of human cancer cell growth and metastasis in nude mice by oral intake of modified citrus pectin. *J Natl Cancer Inst* 2002;94(24):1854–62.
- Gunning AP, Bongaerts RJ, Morris VJ. Recognition of galactan components of pectin by galectin-3. *Faseb J* 2009;23(2):415–24.
- Streetly MJ, Maharaj L, Joel S, Schey SA, Gribben JG, Cotter FE. GCS-100, a novel galectin-3 antagonist, modulates MCL-1, NOXA, and cell cycle to induce myeloma cell death. *Blood* 2010;115:3939–48.
- Gao X, Zhi Y, Sun L, Peng X, Zhang T, Xue H, Tai G, Zhou Y. The inhibitory effects of a rhamnogalacturonan I (RG-I) domain from ginseng pectin on galectin-3 and its structure-activity relationship. *J Biol Chem* 2013;288(47):33953–65.
- Zhang L, Wang P, Qin Y, Cong Q, Shao C, Du Z, Ni X, Li P, Ding K. RN1, a novel galectin-3 inhibitor, inhibits pancreatic cancer cell growth in vitro and in vivo via blocking galectin-3 associated signaling pathways. *Oncogene* 2017;36:1297–308.
- Xue H, Zhao Z, Lin Z, Geng J, Guan Y, Song C, Zhou Y, Tai G. Selective effects of ginseng pectins on galectin-3-mediated T cell activation and apoptosis. *Carbohydr Polym* 2019;219:121–9.
- Zhou L, Ma P, Shuai M, Huang J, Sun C, Yao X, Chen Z, Min X, Zhang T. Analysis of the water-soluble polysaccharides from Camellia japonica pollen and their inhibitory effects on galectin-3 function. *Int J Biol Macromol* 2020;159:455–60.
- Pan X, Wang H, Zheng Z, Huang X, Yang L, Liu J, Wang K, Zhang Y. Pectic polysaccharide from Smilax China L. ameliorated ulcerative colitis by inhibiting the galectin-3/NLRP3 inflammasome pathway. *Carbohydr Polym* 2022;277:118864.
- Hadari YR, Arbel-Goren R, Levy Y, Amsterdam A, Alon R, Zakut R, Zick Y. Galectin-8 binding to integrins inhibits cell adhesion and induces apoptosis. *J Cell Sci* 2000;113:2385–97.
- Stowell SR, Arthur CM, Slanina KA, Horton JR, Smith DF, Cummings RD. Dimeric Galectin-8 induces phosphatidylserine exposure in leukocytes through polylectosamine recognition by the C-terminal domain. *J Biol Chem* 2008;283(29):20547–59.
- Ideo H, Matsuzaka T, Nonaka T, Seko A, Yamashita K. Galectin-8-N-domain recognition mechanism for sialylated and sulfated glycans. *J Biol Chem* 2011;286(13):11346–55.
- Troncoso MF, Ferragut F, Bacigalupo ML, Cardenas Delgado VM, Nugnes LG, Gentilini L, Laderach D, Wolfenstein-Todel C, Compagno D, Rabinovich GA, Eloia MT. Galectin-8: a matricellular lectin with key roles in angiogenesis. *Glycobiology* 2014;24(10):907–14.
- Stowell SR, Arthur CM, Dias-Baruffi M, Rodrigues LC, Gouridine JP, Heimbürg-Molinari J, Ju T, Molinaro RJ, Rivera-Marrero C, Xia B, Smith DF, Cummings RD. Innate immune lectins kill bacteria expressing blood group antigen. *Nat Med* 2010;16(3):295–301.
- Norambuena A, Metz C, Vicuna L, Silva A, Pardo E, Oyanadel C, Massardo L, Gonzalez A, Soza A. Galectin-8 induces apoptosis in Jurkat T cells by phosphatidic acid-mediated ERK1/2 activation supported by protein kinase A down-regulation. *J Biol Chem* 2009;284(19):12670–9.
- Zhang M, Zu H, Zhuang X, Yu Y, Wang Y, Zhao Z, Zhou Y. Structural analyses of the HG-type pectin from notopterygium incisum and its effects on galectins. *Int J Biol Macromol* 2020;162:1035–43.
- Stegmayr J, Lepur A, Kahl-Knutson B, Aguilar-Moncayo M, Klyosov AA, Field RA, Oredsson S, Nilsson UJ, Leffler H. Low or No inhibitory potency of the canonical galectin carbohydrate-binding site by pectins and galactomannans. *J Biol Chem* 2016;291(25):13318–34.
- Si Y, Wang Y, Gao J, Song C, Feng S, Zhou Y, Tai G, Su J. Crystallization of galectin-8 linker reveals intricate relationship between the N-terminal tail and the linker. *Int J Mol Sci* 2016;17(12):2088.
- Zhang T, Zheng Y, Zhao D, Yan J, Sun C, Zhou Y, Tai G. Multiple approaches to assess pectin binding to galectin-3. *Int J Biol Macromol* 2016;91:994–1001.

- [33] Xue H, Liu L, Zhao Z, Zhang Z, Guan Y, Cheng H, Zhou Y, Tai G. The N-terminal tail coordinates with carbohydrate recognition domain to mediate galectin-3 induced apoptosis in T cells. *Oncotarget* 2017;8:49824–38.
- [34] Mohnen D. Pectin structure and biosynthesis. *Curr Opin Plant Biol* 2008;11(3): 266–77.
- [35] Ding H, Cui S, Goff H, Chen J, Wang Q, Han N. Arabinan-rich rhamnogalacturonan-I from flaxseed kernel cell wall. *Food Hydrocolloids* 2015;47:158–67.
- [36] Guo Q, Cui SW, Kang J, Ding H, Wang Q, Wang C. Non-starch polysaccharides from American ginseng: physicochemical investigation and structural characterization. *Food Hydrocolloids* 2015;44:320–7.
- [37] Norambuena A, Metz C, Vicuna L, Silva A, Pardo E, Oyanadel C, Massardo L, Gonzalez A, Soza A. Galectin-8 induces apoptosis in Jurkat T cells by phosphatidic acid-mediated ERK1/2 activation supported by protein kinase A down-regulation. *J Biol Chem* 2009;284:12670–9.
- [38] Zhang T, Lan Y, Zheng Y, Liu F, Zhao D, Mayo KH, Zhou Y, Tai G. Identification of the bioactive components from pH-modified citrus pectin and their inhibitory effects on galectin-3 function. *Food Hydrocolloids* 2016;58:113–9.
- [39] Mariño KV, Cagnoni AJ, Croci DO, Rabinovich GA. Targeting galectin-driven regulatory circuits in cancer and fibrosis. *Nat Rev Drug Discov* 2023;22:295–316.
- [40] Kruk L, Braun A, Cosset E, Gudermann T, Mammadova-Bach E. Galectin functions in cancer-associated inflammation and thrombosis. *Front Cardiovasc Med* 2023;10:1052959. <https://doi.org/10.3389/fcvm.2023.1052959>.